Analyst

Accepted Manuscript

ROYAL SOCIETY OF CHEMISTRY

www.rsc.org/analyst

Striatal dopamine release in a schizophrenia mouse model measured by electrochemical amperometry *in vivo*

Huadong Xu[1,3], Panli Zuo[1,3], Shirong Wang[1,3], Li Zhou[1], Xiaoxuan Sun[1], Meiqin Hu[1], Bin Liu[1], Qihui Wu[1], Haiqiang Dou[1], Bing Liu[1], Feipeng Zhu[1], Sasa Teng[1], Xiaoyu Zhang[1], Li Wang[1], Qing Li[1], Mu Jin[1], Xinjiang Kang[1], Wei Xiong[2], Changhe Wang[1,4], and Zhuan Zhou[1, 4]

[1]State Key Laboratory of Biomembrane and Membrane Biotechnology and Beijing Key Laboratory of Cardiometabolic Molecular Medicine, Institute of Molecular Medicine and PKU-IDG/McGovern Institute for Brain Research and Peking-Tsinghua Center for Life Sciences, Peking University, Beijing 100871, China;

[2]THU-IDG/McGovern Institute for Brain Research, School of Life Sciences, Tsinghua University, Beijing 100084, China

[3]Equal contributors

[4]Correspondence authors (ZZ: zzhou@pku.edu.cn ; CHW: changhecool@163.com)

Abbreviated title: Striatal dopamine in a schizophrenia mouse *in vivo*

Key Words: dysbindin, striatum, schizophrenia, amperometry, in vivo dopamine recording

Address for editorial correspondence and proof:

Dr. Zhuan Zhou
Institute of Molecular Medicine
Peking University,
Beijing 100871
China
Tel & Fax: ++86-10-6275-3212
email: zzhou@pku.edu.cn
http://www.imm.pku.edu.cn/

Abstract

Schizophrenia is a severely devastating mental disorder, the pathological process of which is proposed to be associated with the dysfunction of dopaminergic transmission. Our previous results have demonstrated slower kinetics of transmitter release (glutamate release in hippocampus and norepinephrine release in adrenal slice) in a schizophrenia model, *dysbindin* null-*sandy* mice[1]. However, whether dopaminergic transmission in nigrostriatal pathway is contributing to the pathology in *dysbindin*-/- mouse remains unknown. Here, we provided a step-by-step protocol to apply *in vivo* amperometric recording of dopamine (DA) release from mouse striatum evoked by an action potential (AP) pattern. With this protocol, AP pattern-dependent DA release was recorded from *dysbindin*-/- mice striatum *in vivo*. Combining with amperometric recording in slice and electrophysiology, we found that, in *dysbindin* -/- mice, (1) presynapticlly, AP-pattern dependent dopamine overflow and uptake were intact *in vivo*; (2) the recycling of dopamine vesicle pool remained unchanged. (3) Postsynapticlly, the excitability of medium spine neuron (MSN) was also normal, as revealed by patch-clamp recordings in striatal slices. Taken together, in contrast to reduced norepinephrine release in adrenal chromaffin cells, the dopaminergic transmission remain unchanged in nigrostriatal pathway in *dysbindin*-/- mice, implicating a new insight for function of the schizophrenia susceptibility gene *dysbindin*.

Introduction

Schizophrenia is a pervasive debilitating neuropsychiatric disease, which is characterized by symptoms of delusion, cognitive deficit and mental disorder, affecting ~1% of the worldwide population. Genetic studies show that the heritability of schizophrenia is quite high[2], and several susceptibility genes have been identified[3]. Among these, one of the most famous gene dystrobrevin-binding protein 1 (short as *dysbindin*, also known as *DTNBP1* in humans) has been found highly associated with schizophrenia[4, 5]. DBA/2J strain mouse contains a spontaneous deletion in the gene *dysbindin*, which is named *sandy* mouse[6, 7]. Later, *dysbindin*-/- mice are derived from the *sandy* mice[8]. Currently, the *sandy* or *dysbindin*-/- mouse becomes a well-established model for studying schizophrenia.

With the discovery of the schizophrenia susceptibility gene *dysbindin*, collective evidences have shown that dysbindin deficit leads to the false dopaminergic transmission. It is reported that knockdown of dysbindin in cultured PC12 cells induces increased dopamine (DA) release by up-regulating SNAP25 (synaptosomal-associated protein, 25kDa) expression[9]. Regarding the postsynaptic neurons, it is reported that plasma membrane-located dopamine D2 receptor are altered in prefrontal cortical neurons of *dysbindin*-/- mice[8]. Noticeably, recent studies prompted that dopaminergic transmission in striatum contributed to the cognitive symptoms of schizophrenia[10, 11]. Thus, whether the DA transmission is changed in dysbindin-/- striatum remains unclear.

Unambiguous and precise assessment of DA release requires real-time

measurement of DA in striatum *in vivo*, and such requirement was met by electrochemical recording (amperometry or fast scan cyclic voltammetry) *in vivo* with carbon fiber electrode (CFE)[12, 13]. The amperometric recording provides millisecond temporal-resolution measurement, which permits the precise assessment of DA release and reuptake.

Here, by combining electrochemical recording and electrophysiology, we studied the dopaminergic transmission in schizophrenia-related nigrostriatal pathway of *dysbindin*-/- mice. Our data demonstrated that DA release, reuptake, and vesicle pool recycling, as well as the postsynaptic medium spine neuron (MSN) excitability were intact in *dysbindin*-/- mice.

Experimental

Animals and materials

The *dysbindin*-/- mice with C57BL/6 background were gift from Bai Lu[8]. The mice were kept in animal center of Peking University with 12h light/dark cycle. Food and water were supplied *ad libitum*. The room temperature was maintained at 22-25 °C. All procedures were approved and performed according to the guidelines of the Peking University Animal Use and Care Committee and the Association for Assessment and Accreditation of Laboratory Animal Care. 2-3 months' wild type (WT) and *dysbindin*-/- littermates were used for electrochemical experiments, while 20-30 days for electrophysiology experiments. The mice were anesthetized with urethane (1.5 g/kg, *i.p.*) for *in vivo* and *in vitro* experiment. All chemicals were purchased from Sigma-Aldrich (St. Louis, USA) unless otherwise indicated.

In vivo electrochemistry

The anesthetized mice were fixed on a stereotaxic instrument (Narishige, Japan). Body temperature was monitored and maintained at 37°C with a heating pad (KEL-2000, Nanjing, China). DA overflow was recorded in mouse dorsal striatum i*n vivo* by electrochemical carbon fiber electrode (CFE) as previously described in rat[12]. A bipolar stimulating electrode was implanted in the medial forebrain bundle (MFB: 2.1 mm AP, 1.1 mm ML, 4.0-5.0 mm DV). The recording CFE electrode was implanted in caudate-putamen of dorsal striatum (CPu: 1.1 mm AP; 1.7 mm ML, ~3.4 mm DV). An Ag/AgCl reference electrode was placed in the contralateral cortex. Electric stimulation was generated by an isolator (A395, WPI, USA) as a train of

several biphasic square-wave pulses (0.6 mA, 1 ms duration). The CFE was hold at 780 mV to oxidize the substance in amperometry. Amperometric signal was amplified by a patch-clamp amplifier (PC2C, INBIO, Wuhan, China), low pass-filtered at 50 Hz and recorded by MBA-1 software (INBIO, Wuhan, China) (Supplementary Fig. 1). In this work, amperometry is used to record dopamine release following MFB stimulation for its superior temporal resolution and higher signal-to-noise ratio. To confirm that dopamine is underlining the amperometric current, fast scan cyclic voltammetry was performed by EPC9/2 amplifier and Patch master software (HEKA Electronic, Lambrecht/Pfalz, Germany) as described previously.[12, 14]

Striatal slice preparation

The anesthetized mice were perfused with ~20 ml ice-cold artificial cerebrospinal fluid (cutting aCSF) containing (in mM): 110 $C_5H_{14}NClO$, 2.5 KCl, 0.5 $CaCl_2$, 7 $MgCl_2$, 1.3 NaH_2PO_4, 25 $NaCO_3$, 25 glucose (saturated with 95% O_2 and 5% CO_2). Then the brain was rapidly taken out, and 300 μm-thick coronal striatal slices were cut on a vibratome (Leica VT 1000S, Nussloch, Germany). Slices were incubated for 30 min in recording aCSF (in mM): 125 NaCl, 2.5 KCl, 2 $CaCl_2$, 1.3 $MgCl_2$, 1.3 NaH_2PO_4, 25 $NaCO_3$, 10 glucose (saturated with 95% O_2 and 5% CO_2) at 37°C, and then kept at room temperature for recording.

Striatal slice electrochemistry

Electrochemical recording assay in striatal slices was slightly modified from our previous work[14, 15]. Experiment was performed on an electrophysiology setup. The CFE was inserted into the slice until the CFE tip (~200 μm) was completely inserted

in the dorsolateral caudate region of the striatum. Electrical stimuli were delivered by a bipolar electrode (Plastics One Inc., USA), and electrical stimulation was generated by a Grass S88K stimulator (Astro-Med, USA). The pulses were given at 0.2 ms of duration, 0.6 mA of amplitude and 3 min of interval. Amperometric signals were recorded with an EPC9/2 amplifier and Pulse software (HEKA Electronic, Lambrecht/Pfalz, Germany).

Striatal slice electrophysiology

Whole-cell recordings were performed on MSN located in the dorsal striatum. MSN was identified by its smaller diameters (~10 μm) and lower rest potential at -80 mV. Briefly, cells were current-clamped with a pipette electrode controlled by the EPC9/2 amplifier. The pipette resistance was controlled between 4-5 MΩ, and the electrode was filled with a 10 mM K^+-containing intracellular solution (in mM): 130 K gluconate, 10 KCl, 2 $MgCl_2$, 2.5 Mg-ATP, 0.25 Na-GTP, 10 HEPES, and 0.4 EGTA, pH 7.3.

Data analysis

Data were analyzed with IGOR Pro software (WaveMetrics, USA). Especially, artifact and noise of DA signal *in vivo* are processed in Igor software (Supplementary Fig. 2). Data are shown as mean ± s.e.m. Statistical comparisons were performed with the two-tailed unpaired Student's *t*-test, and all tests were conducted using SPSS (version 13.0, Statistical Package for the Social Sciences). Significant differences were accepted at $P < 0.05$.

Results and Discussion

Amperometric recording of DA overflows in anesthetic mice striatum *in vivo*

Usually, *in vivo* amperometry system is composed of a recording system and a stimulation system. The recording system includes an amplifier, a filter and an AD/DA converter. A computer generates stimuli through the AD/DA converter and an isolator (Fig. 1A, for setup details, see supplemental information). The CFE (recording) and bipolar stimulation electrodes were inserted into the striatum and the MFB of the anesthetized mouse respectively (Fig .1 B, for detailed protocol, see supplemental Fig. 1). A burst of pulses stimulus was applied to trigger DA release in striatum, and the optimal signals were obtained by adjusting the depth of both electrodes. For instance, a burst stimulation of 36 pulses at 80 Hz triggered a ~400 pA oxidation current (the trace was processed with lab-made macro in Igor Pro, see supplemental Fig. 2), followed by a fast decay with a velocity of ~750 pA/s (linear fitted V_{max}) (Fig. 1C), which represented the uptake velocity of DA transporter (DAT). Half-height duration (HHD, ~ 0.6 s) of the oxidation current is also a significant parameter to speculate the kinetics of DA overflows.

To determine that the recorded signals by amperometry *in vivo* were DA signals, a fast-scan cyclic voltammetry (FSCV) were also used (for details see supplemental Fig. 3). In FSCV voltammogram, the oxidization and reduction currents peaked at 620 mV and -230 mV for *in vivo* recording respectively, which was consistent with the voltage peaks obtained in DA solution *in vitro* (Fig. 1D). In addition, the results were confirmed by microdialysis-based high performance liquid chromatography (HPLC) (data not shown).

Stimulus codes for estimation of DA release properties

To mimic the *in vivo* neural activities during physiological conditions, the AP pattern of stimulation was defined by four codes [N, f, b, i], in which N was the total number of APs, f was the AP frequency in each burst, b represented the burst number, and i represented the inter-burst interval (Fig. 2A)[12]. Using a fixed number of APs for 1 burst ([36, f, 1, 0 s]), we found that DA overflow in striatum was dependent on the stimulus frequency, which reached the peak value at 80 Hz (Fig. 2B and C). The sustainability of DA release was estimated by the ratio of the n^{th} to 1^{st} amplitudes (A_n/A_1) in DA overflow evoked by a burst stimulation of [144, 80 Hz, b4, 1s] (Fig. 2 D and E). A ratio of 0.6 derived by A_4 and A_1 indicated there was little depletion in the DA releasable vesicle pools.

Intact DA overflows and release sustainability in *dysbindin*-/- striatum *in vivo*

We have reported that the kinetics of vesicle fusion become slower and the total norepinephrine (NE) release is reduced in adrenal chromaffin cells of adrenal slices in *dysbindin* -/- mice (Fig. 3E, left panel)[1]. As dysbindin is ubiquitously expressed in brain and dysfunction of DA release in striatum is associated with pathological process of schizophrenia, we investigated whether DA release in nigrostriatal pathway was altered in *dysbindin*-/- mouse.

In contrast to the decreased NE release in adrenal slices and glutamate release in hippocampal neurons[1], the amplitude and integral of evoked dopamine overflow remained unchanged in *dysbindin*-/- mice (Fig. 3B, left panel: WT, 423±63.9 pA; *dysbindin*-/-, 515±49.6 pA; P = 0.92; Fig. 3E, right panel: WT, 287±48 pC;

dysbindin-/-, 300±48 pC; P = 0.79). In addition, no differences of HHD (Fig. 3B, middle panel: WT, 0.65 ± 0.04 s; *dysbindin*-/-, 0.70 ± 0.03 s, P = 0.29) and V_{max} (Fig. 3B, right panel: WT, 735±85.2 pA/s; *dysbindin*-/- mice, 625±43.1 pA/s, P = 0.22) were found between *dysbindin*-/- and WT mice, indicating the normal DAT function in *dysbindin*-/- mice. Taken together, these results demonstrated that both DA release and uptake were intact in the striatum of *dysbindin*-/- mice. Dysbindin also plays a critical role in the vesicle trafficking[8, 16], thus we assessed the sustainability of DA release *in vivo* (Fig. 3C). The A_n/A_1 remained unchanged during the four bursts of pulses stimulation in *dysbindin*-/- mice (Fig. 3E), indicating the unchanged sustainability of DA release or DA vesicle trafficking in striatum in *dysbindin*-/- mice *in vivo*.

Intact DA release in *dysbindin*-/- striatal slices

To confirm the unchanged DA release in *dysbindin*-/- mice revealed by *in vivo* experiment, we also compared dopamine signals in striatal slices. Consistent with *in vivo* results, the amplitude of evoked DA release was similar in WT and *dysbindin*-/- mice in response to single pulse stimulation (Fig. 5D, left panel: WT, 217 ± 20.2 pA, n = 10 slices from 3 mice; *dysbindin*-/-, 178 ± 21.3 pA, n = 13 slices from 3 mice; P = 0.2). The charge of DA overflow also remained unchanged in *dysbindin*-/- mice (Fig. 5D right panel: WT, 40 ± 6.9 pC; *dysbindin*-/-, 36.7 ± 2.7 pC, P = 0.65), confirming the intact DA release and uptake in striatum in *dysbindin*-/- mice. To examine the recycling of DA releasable vesicle pool of *dysbindin*-/- mice, we recorded the DA release in response to the paired-pulse stimulation, and paired-pulse

ratio (PPR) of DA current (A_2/A_1) was used to evaluate the DA vesicle pool recycling (Fig. 5C). There is no significant difference of the PPRs between WT and *dysbindin*-/- mice at all intervals (WT, n = 6 slices from 2 mice; *dysbindin*-/-, n = 6 slices from 3 mice; $P > 0.05$ at each time point), and the recycling time constant for WT and *dysbindin*-/- mice were τ_{WT} = 16.9 s and $\tau_{dysbindin-/-}$ = 18.5 s. Taken together, these findings confirmed the normal DA release and vesicle recycling in striatum in *dysbindin*-/- mice.

Dopaminergic transmission includes presynaptic DA release and response of postsynaptic neurons to DA input. Since there was no dramatic difference of presynaptic DA release in *dybindin*-/- striatum, we then investigated whether the function of postsynaptic medium spine neurons (MSN) was altered in *dybindin*-/- mice using whole cell current-clamp in striatal slices. The MSNs were identified by the size of cell body (~10 μm in diameter) and the resting potential (~- 80 mV, Fig. 6B). An 800-ms long depolarization step was applied to induce action potentials under current-clamp mode. The firing frequencies of action potentials increased in response to the increased injected-currents (Fig. 6A and C). However, the depolarization-induced spike numbers remained similar between WT and *dysbindin*-/- mice (Fig. 6C, WT, n = 8 cells; *dysbindin*-/-, n = 11 cells, $P > 0.05$ at each point). Therefore, *dysbindin* null mutation did not change the excitability of MSN in striatum dramatically. However, we still couldn't exclude the possible alteration of the other interneurons, including fast-spiking interneurons, low-threshold spiking interneurons, and cholinergic interneurons [17].

Conclusion

Confirmed by FSCV and microdialysis-based HPLC, the *in vivo* amperometry is an excellent method to identify the dysfunction of DA transmission in animal disease models. FSCV and HPLC possess the advantage in identifying substance, but amperometry has higher temporal and spatial resolution[14, 18]. In the present study, we systematically analyzed DA release, uptake and vesicle pool recycling in striatal dopaminergic terminals and of *dysbindin*-/- mice *in vivo* and in slices, and found the normal function of presynaptic DA release as well as its postsynaptic neurons (MSN). Taken together, in contrast to the altered release of transmitters in adrenal and hippocampus, our results demonstrated that striatal DA signal is not altered in the schizophrenia model of *dysbindin*-/- mice, implicating the novel insight of the schizophrenia susceptibility gene *dysbindin* in the striatum.

ACKNOWLEDGEMENTS

We thank Bai Lu for *dysbindin-/-* mice and Bo Feng for helping Igor macro software. This work was supported by grants from the National Basic Research Program of China (2012CB518006), the National Natural Science Foundation of China (31228010，31171026, 31100597, 31327901，81222020, 31221002, and 31330024), the National Key Technology R&D Program (SQ2011SF11B01041), and a “985” grant from the Department of Education of China.

Author Contributions: H.X., P.Z., S.W., L.Z., X.S., M.H., B.L., Q.W., H.D., B.L.,

F.Z., S.T., X.Z., L.W., Q.L., M.J., and X.K. performed experiments. C.W., and Z.Z. designed the work, H.X., S.W., P.Z., W.X., C.W., and Z.Z. wrote the manuscript.

References:

1. X. W. Chen, Y. Q. Feng, C. J. Hao, X. L. Guo, X. He, Z. Y. Zhou, N. Guo, H. P. Huang, W. Xiong, H. Zheng, P. L. Zuo, C. X. Zhang, W. Li and Z. Zhou, *J Cell Biol*, 2008, 181, 791-801.
2. A. G. Cardno and Gottesman, II, *Am J Med Genet*, 2000, 97, 12-17.
3. N. Norton, H. J. Williams and M. J. Owen, *Curr Opin Psychiatry*, 2006, 19, 158-164.
4. R. E. Straub, Y. Jiang, C. J. MacLean, Y. Ma, B. T. Webb, M. V. Myakishev, C. Harris-Kerr, B. Wormley, H. Sadek, B. Kadambi, A. J. Cesare, A. Gibberman, X. Wang, F. A. O'Neill, D. Walsh and K. S. Kendler, *Am J Hum Genet*, 2002, 71, 337-348.
5. S. G. Schwab, M. Knapp, S. Mondabon, J. Hallmayer, M. Borrmann-Hassenbach, M. Albus, B. Lerer, M. Rietschel, M. Trixler, W. Maier and D. B. Wildenauer, *Am J Hum Genet*, 2003, 72, 185-190.
6. R. T. Swank, H. O. Sweet, M. T. Davisson, M. Reddington and E. K. Novak, *Genet Res*, 1991, 58, 51-62.
7. W. Li, Q. Zhang, N. Oiso, E. K. Novak, R. Gautam, E. P. O'Brien, C. L. Tinsley, D. J. Blake, R. A. Spritz, N. G. Copeland, N. A. Jenkins, D. Amato, B. A. Roe, M. Starcevic, E. C. Dell'Angelica, R. W. Elliott, V. Mishra, S. F. Kingsmore, R. E. Paylor and R. T. Swank, *Nat Genet*, 2003, 35, 84-89.
8. Y. Ji, F. Yang, F. Papaleo, H. X. Wang, W. J. Gao, D. R. Weinberger and B. Lu, *Proc Natl Acad Sci U S A*, 2009, 106, 19593-19598.
9. N. Kumamoto, S. Matsuzaki, K. Inoue, T. Hattori, S. Shimizu, R. Hashimoto, A. Yamatodani, T. Katayama and M. Tohyama, *Biochem Biophys Res Commun*, 2006, 345, 904-909.
10. A. Sawa and S. H. Snyder, *Science*, 2002, 296, 692-695.
11. E. H. Simpson, C. Kellendonk and E. Kandel, *Neuron*, 2010, 65, 585-596.
12. S. R. Wang, W. Yao, H. P. Huang, B. Zhang, P. L. Zuo, L. Sun, H. Q. Dou, Q. Li, X. J. Kang, H. D. Xu, M. Q. Hu, M. Jin, L. Zhang, Y. Mu, J. Y. Peng, C. X. Zhang, J. P. Ding, B. M. Li and Z. Zhou, *J Neurochem*, 2011, 119, 342-353.
13. A. G. Ewing, J. C. Bigelow and R. M. Wightman, *Science*, 1983, 221, 169-171.
14. L. Wang, X. Zhang, H. Xu, L. Zhou, R. Jiao, W. Liu, F. Zhu, X. Kang, B. Liu, S. Teng, Q. Wu, M. Li, H. Dou, P. Zuo, C. Wang, S. Wang and Z. Zhou, *J Physiol*, 2014, 592, 3559-3576.
15. H. P. Huang, S. R. Wang, W. Yao, C. Zhang, Y. Zhou, X. W. Chen, B. Zhang, W. Xiong, L. Y. Wang, L. H. Zheng, M. Landry, T. Hokfelt, Z. Q. Xu and Z. Zhou, *Proc Natl Acad Sci U S A*, 2007, 104, 1401-1406.
16. A. Marley and M. von Zastrow, *PLoS One*, 2010, 5, e9325.
17. A. C. Kreitzer, *Annu Rev Neurosci*, 2009, 32, 127-147.
18. X. Kang, H. Xu, S. Teng, X. Zhang, Z. Deng, L. Zhou, P. Zuo, B. Liu, B. Liu, Q. Wu, L. Wang, M. Hu, H. Dou, W. Liu, F. Zhu, Q. Li, S. Guo, J. Gu, Q. Lei, J. Lu, Y. Mu, M. Jin, S. Wang, W. Jiang, K. Liu, C. Wang, W. Li, K. Zhang and Z. Zhou, *Proc Natl Acad Sci U S A*, 2014, DOI: 10.1073/pnas.1408484111.
19. P. E. Phillips, G. D. Stuber, M. L. Heien, R. M. Wightman and R. M. Carelli, *Nature*, 2003, 422, 614-618.

Fig. 1 Methodology of electric-chemical amperometry recording of DA overflows in anesthetic mice striatum *in vivo.*

(A) Circuit diagram for the *in vivo* amperometric recording system. (B) Diagram of electrodes positions in DA overflow recording in mouse striatum *in vivo*. (C) An example trace for DA overflow (I_{amp}) following 36 stimulus pulses at 80 Hz applied to the MFB. Amplitude, HHD and V_{max} are defined as illustrated. (D) DA signals detected by fast scan cyclic voltammetry (FSCV) *in vivo*. Left panel, time course of DA overflow signal (I_{FSCV}-*t* curve) derived from FSCV recordings at 620 mV. Insert, representative FSCV voltammograms of DA signal in striatum *in vivo* (black line) and 5 μM DA solution in vitro (Dashed gray line). Right panel, corresponding I_{FSCV}–*V*–*t* pseudocolour plot [19] to the left I_{FSCV}.

Fig. 2 Stimulus codes for estimating of DA release properties

(A) Diagram of a typical multiple-bursts stimulus pattern [144, 80 Hz, b4, 1s], insert shows part of a burst at expanded scale. (B) DA signals in response to 36 APs at various frequencies ranged from 20 to 100Hz. (C) Statistic results for the amplitude of DA overflow at different frequency (n=7). (D) Representative trace of DA overflow in response to multiple AP bursts stimuli [144, 80 Hz, b4, 1s], A_1 to A_4 representing the amplitude of evoked DA signal during each burst. (E) Statistic results of A_n/A_1 in DA overflows (n=4).

Fig. 3 Intact DA overflows and release sustainability in *dysbindin*-/- mice striatum *in vivo*

(A) Representative amperometric recording traces of DA overflow in WT (grey, left) and *dysbindin*-/- mice (black, right) in response to [36, 80 Hz] stimulation. (B) Statistic results of amplitude, HHD and V_{max} of DA overflow shows no significant difference in WT and *dysbindin*-/- mice (WT, n=7; *dysbindin*-/-, n=10). (C) Representative amperometric recording traces of DA overflow in response to [144, 80 Hz, b4, 1s] stimulation in WT (grey, left) and *dysbindin*-/- mice (black, right). (D) Comparison of ratio (A_n/A_1) for DA overflow between WT and *dysbindin*-/- mice (WT, n=5; *dysbindin*-/-, n=6) (E) Comparison showing reduced NE release in adrenal slice in *sandy* mice[1] and normal DA release in *dysbindin*-/- striatum *in vivo*. $\int I_{amp} dt$ represents the integral of NE signal in adrenal slice (left panel) or the integral of DA signal (Fig. 3A).

Fig. 4 Unchanged dopamine release and vesicle pool recycling in *dysbindin*-/- striatal slice

(A) Photomicrograph showing amperometric recording of E-stim (electric stimulation) evoked DA signals in striatal slices (bar, 100 μm). CFE and twisted stimulation electrode were placed as illustrated. (B) Representative amperometric trace of dopamine overflow in response to a single pulse stimulation in WT (grey) and *dysbindin*-/- mice (black). (C) Representative traces of DA overflow in response to paired pulse stimulations at 4 s interval in WT (grey) and *dysbindin*-/- (black) striatal slice (A_1 was normalized to 1 for comparison). (D) Quantitative analysis of amplitude and charge of dopamine overflow in WT and *dysbindin*-/- mice (13 slices from 3 WT

mice, 10 slices from 3 *dysbindin*-/- mice, P>0.05). (E) Time courses of DA vesicle pool recycling between WT and *dysbindin*-/- mice, presented as PPR at interval time ranging from 1s to 100s (WT, 6 slices from 2 mice; *dysbindin*-/-, 6 slices from 3 mice). Data were fitted by single exponential functions. (Grey lines for WT mice, black lines for *dysbindin*-/- mice). τ_{WT}, recycling time constant for WT mice, $\tau_{dysbindin-/-}$, recycling time constant for *dysbindin*-/- mice.

Fig. 5 Normal excitability of MSN in striatal slice in *dysbindin*-/- mice

(A) Representative action potentials (AP) of MSNs in response to current injection (current intensity ranging from 250 to 400 pA; length 800 ms) in current-clamped model in WT and *dysbindin*-/- striatal slices. (B) Photomicrograph showing the whole cell-patch on medium spine neurons. (C) AP number-current plot indicating intact excitability of MSNs in *dysbindin*-/- mice (WT, 8 cells from 4 mice, *dysbindin*-/-, 11 cells from 3 mice).

Fig. 1:

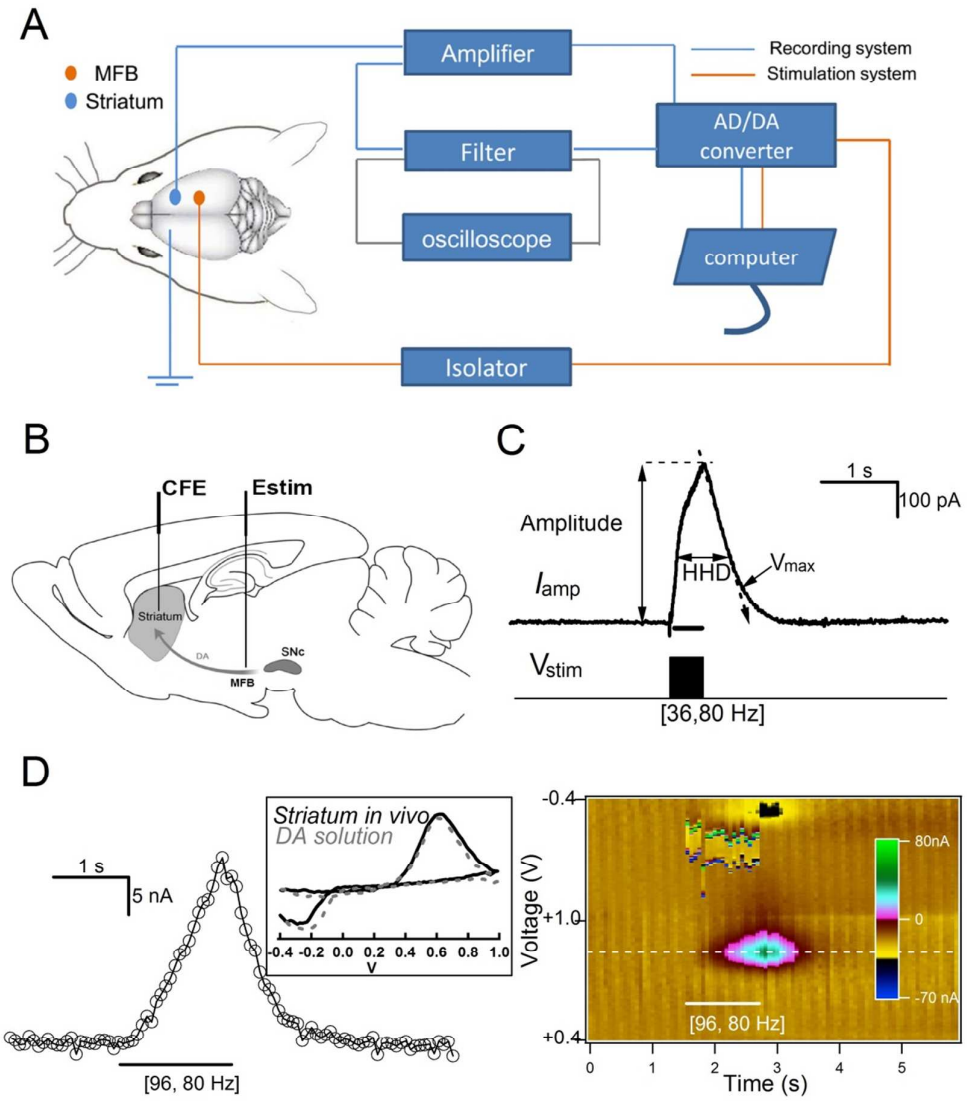

Fig. 2:

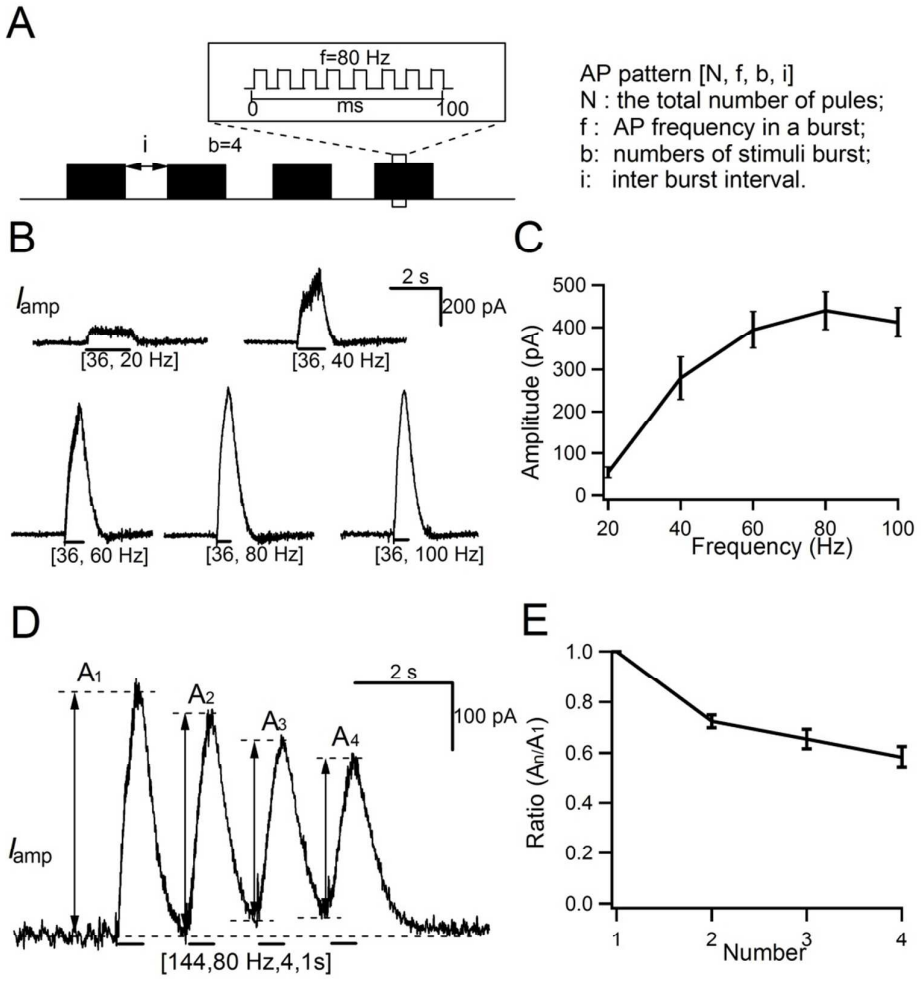

Fig. 3:

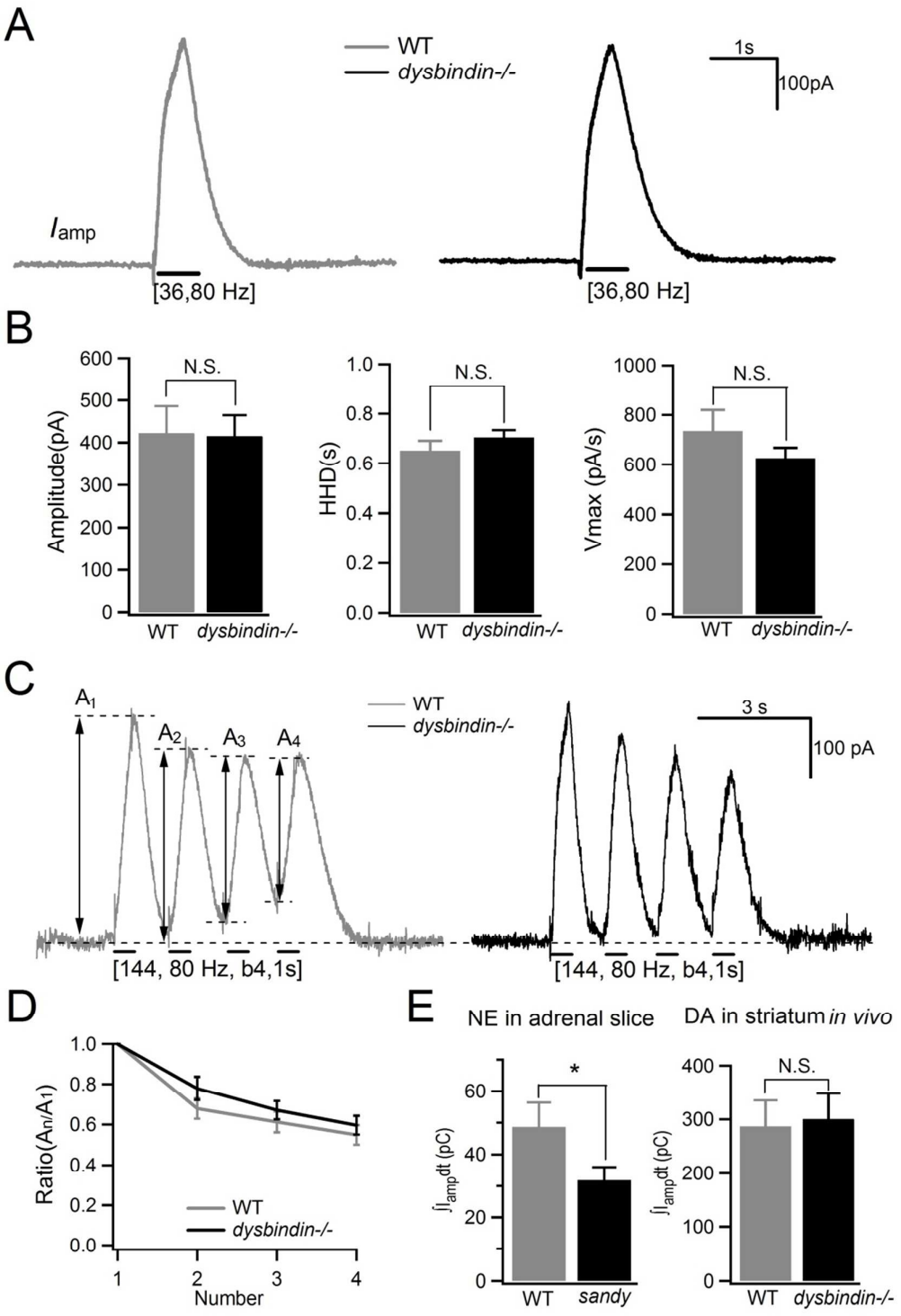

Fig. 4:

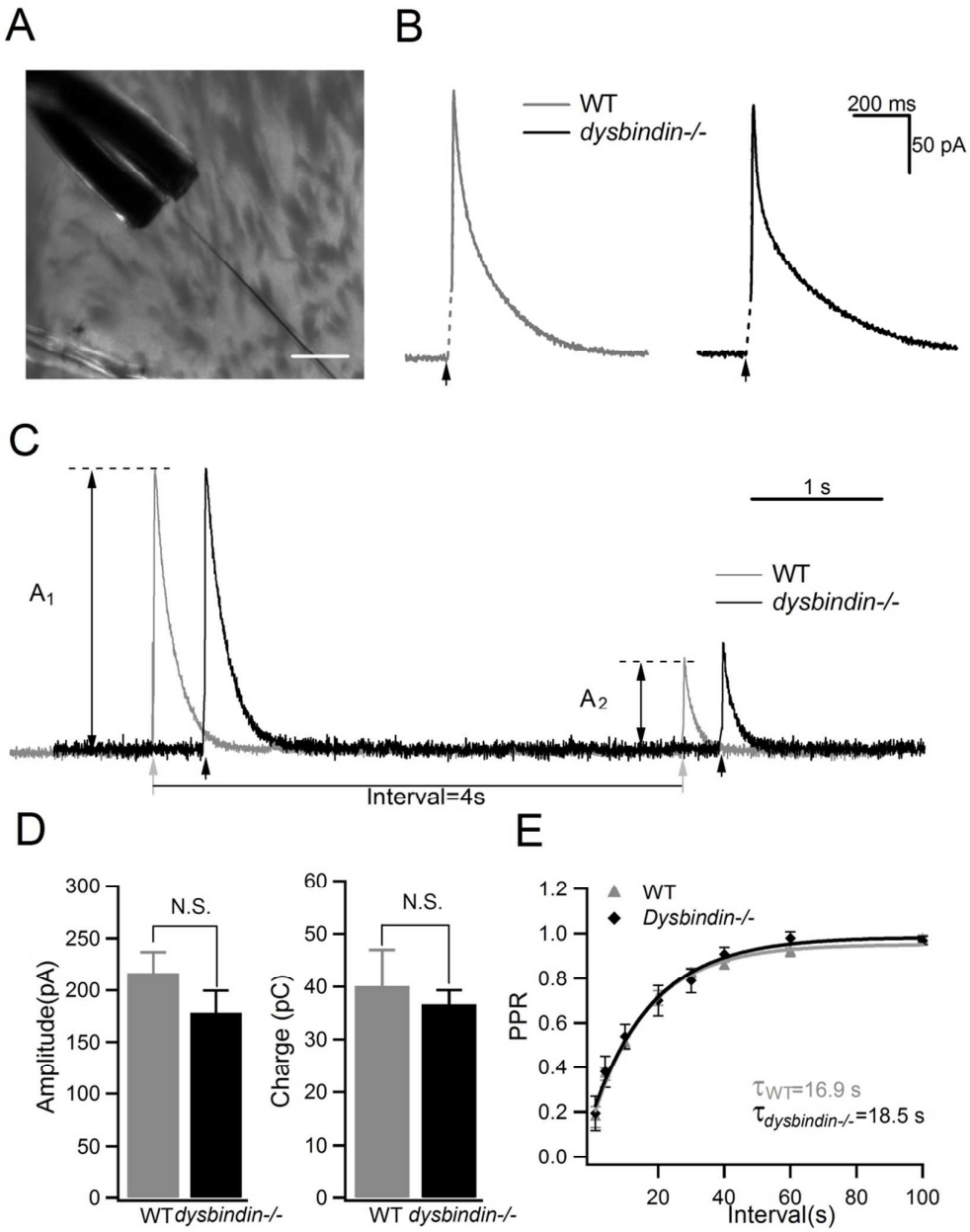

Fig. 5: